Available online at www.sciencedirect.com
ScienceDirect
International Journal of Pharmaceutics 330 (2007) 61–72
INTERNATIONAL JOURNAL OF PHARMACEUTICS
www.elsevier.com/locate/ijpharm

Evaluation of the USP dissolution test method A for enteric-coated articles by planar laser-induced fluorescence

Dave A. Miller [a], Mirko Gamba [b], Dorothea Sauer [a], Troy P. Purvis [a], Noel T. Clemens [b], Robert O. Williams III [a,*]

[a] *College of Pharmacy, The University of Texas at Austin, Austin, TX 78712, United States*
[b] *Department of Aerospace Engineering and Engineering Mechanics, The University of Texas at Austin, Austin, TX 78712, United States*

Received 1 May 2006; received in revised form 26 August 2006; accepted 28 August 2006
Available online 9 September 2006

Abstract

The USP drug release standard for delayed-release articles method A was evaluated using planar laser-induced fluorescence (PLIF). Prior authors have suggested that high pH "hot spots" could develop during the buffer medium addition of the method A enteric test. Additionally, previous studies have shown heterogeneous flow patterns and low-shear regions in the USP Apparatus II dissolution vessel, which may result in poor mixing of the buffer and acid media during the pH neutralization step of the method A enteric test. In this study, PLIF was used to evaluate the mixing patterns and evolution of pH neutralization during the buffer medium addition with rhodamine-B dye and the pH-sensitive dye fluorescein, respectively. Additionally, a comparison of the methods A and B enteric tests was performed with enteric-coated tablets containing rhodamine-B in the film so as to image the dissolution rate of the coating polymer with PLIF in order to determine if rapid buffer addition for the method A procedure accelerates the rate of film coat dissolution. Rapid addition of the 250 mL of buffer medium over 5 s to the 750 mL of acidic medium shows efficient mixing and pH neutralization due to the generation of large-scale stirring and enhanced turbulence resulting from the descending buffer medium. Slow addition near the paddle shaft over 5 min showed segregation in the recirculating region around the paddle shaft. In contrast, slow addition near the vessel wall introduces the medium into fluid outside of the recirculation region and enables transport over the entire vessel. Enteric-coated tablets tested according to method A with rapid medium addition and method B enteric tests performed identically, indicating no difference in polymer dissolution rate between the two tests. From the results of the PLIF imaging studies with rhodamine-B, fluorescein, and enteric-coated tablets, it was seen that "hot spots" affecting the dissolution performance of enteric dosage forms are not generated during the neutralization step of the method A enteric test namely when the media is added rapidly or outside of the recirculating region that surrounds the paddle shaft.

Keywords: Planar laser-induced fluorescence; Dissolution testing; Enteric; Method A; Hot spots

1. Introduction

Polymers with pH-dependent dissolution properties have been investigated extensively for their use in pharmaceutical products intended for delayed drug release (Hasan et al., 1992; Felton et al., 1995; Thoma and Bechtold, 1999; Crotts et al., 2001; Williams, 2001; Bruce et al., 2003a, 2003b). These polymers have been widely used for targeted drug delivery to the small intestine as they allow a drug-containing dosage form to pass through the acidic environment of the stomach intact and with minimal drug release. Enteric polymers, such as various polymethacrylates and cellulose derivatives, exhibit very low solubility in acidic conditions due to free carboxylic acid functional groups on the molecule which remain unionized at low pH. As the pH of the surrounding media increases to a specific value, which varies according to the type and grade of enteric polymer, the functional groups begin to ionize resulting in increased hydrophilicity and solubility. These enteric polymers have been used to protect acid labile drugs from the acidic conditions of the stomach, as well as to prevent gastric irritation that is caused by a variety of drugs (Genc et al., 1997; Schmid et al., 2000; Alavi et al., 2002; Bruce et al., 2003b; Fuerst et al., 2005; Yoo et al., 2005).

* Corresponding author. Tel.: +1 512 471 4681; fax: +1 512 471 7474.
E-mail address: williro@mail.utexas.edu (R.O. Williams III).

0378-5173/$ – see front matter © 2006 Elsevier B.V. All rights reserved.
doi:10.1016/j.ijpharm.2006.08.047

In vitro dissolution testing is essential to evaluate the performance of enteric-coated articles. The methods of analysis described in the USP detail two methods for dissolution testing of enteric products, methods A and B. The method A procedure dictates that the enteric dosage form be tested in 750 mL of 0.1N hydrochloric acid at 37 °C for 2 h (acid phase) followed by the addition of 250 mL of 0.2 M sodium phosphate buffer and any further pH adjustment required to neutralize the pH to approximately 6.8 ± 0.05 within 5 min (buffer phase). With method B, the enteric dosage form is tested in 1 L of 0.1N HCl for 2 h, the vessel is then drained of the acidic medium and filled with 1 L of pH 6.8 phosphate buffer for the buffer phase testing. The performance of enteric articles is evaluated based on drug release during the two phases of the test. A passing enteric test, for six samples, shows less than 10% drug release over 2 h in the acid phase, followed by at least 80% drug release within 45 min following the addition of the buffer medium, or for the time specified for the particular drug product. This *in vitro* test is intended to mimic the passage of an enteric dosage form through the gastrointestinal tract as it first enters the acidic conditions of the stomach followed by movement to the more neutral pH environment of the small intestine.

Inherent in the design of the USP method A enteric test is the assumption that the mixing of the buffer medium with the acid medium, i.e. neutralization of the pH, is sufficiently rapid; that is to say high pH domains that may develop within the dissolution media during the buffer phase addition exist momentarily and do not influence the result of the enteric test. However, it has been suggested that high pH regions existing for non-negligible time periods, termed "hot spots", may occur in the dissolution vessel when enteric dissolution testing is performed according to method A (Hanson and Gray, 2004). Additionally, many researchers have investigated the hydrodynamics of the USP Apparatus II dissolution vessel to find that the mixing environment is non-ideal. The dissolution of USP calibrator tablets was the first attempt to characterize the flow patterns in dissolution vessels (Beckett et al., 1996; King, 1996; Qureshi and Shabnam, 2001; Morihara et al., 2002; Baxter et al., 2005; Mirza et al., 2005). The tablets were placed away from the bottom center of the dissolution vessel using a PEAK^{TM} vessel (Beckett et al., 1996; King, 1996; Mirza et al., 2005), employing a metal strip (Qureshi and Shabnam, 2001), and by tilting the dissolution vessel (Mirza et al., 2005). All studies resulted in higher dissolution rates compared to a standard USP Apparatus II system suggesting the existence of a heterogeneous flow field resulting in a poorly mixed zone at the bottom of the dissolution vessel.

Muzzio and coworkers employed particle imaging velocimetry (PIV) combined with computational fluid dynamics to characterize the entire flow pattern in a USP Apparatus II dissolution vessel at steady state mixing conditions (Kukura et al., 2003, 2004; Baxter et al., 2005). It was seen that an uneven distribution of hydrodynamic forces resulted in a highly non-uniform shear environment throughout the vessel. Increasing the paddle speed from 50 to 100 rpm did not improve shear homogeneity within the dissolution vessel, but rather only increased the shear force. The highest shear was found at the surface of the paddle blade as well as along the vessel walls. Areas of the lowest shear are located above the paddle blade between the paddle shaft and the wall. At the bottom of the USP Apparatus II dissolution vessel, it was seen that a circular low-shear region about the size of a typical dosage-form is produced by the paddle rotation (Kukura et al., 2004). Generally, the hydrodynamics of a dissolution vessel are characterized by areas of recirculating flow patterns. From the paddle, the flow proceeds either up the wall to the liquid surface then descends between the paddle shaft and the wall, or the flow is directed down to the bottom of the vessel ascending back up to the paddle in the center of the dissolution vessel (Baxter et al., 2005). The results of these studies revealed that the USP Apparatus II it is not an ideal mixing device.

In order to characterize accurately the mixing during the neutralization step for the method A enteric test, an experimental technique is required that does not alter the hydrodynamics of the dissolution vessel. Planar laser-induced fluorescence (PLIF) is a widely-used, non-intrusive, planar technique for visualizing the evolution of a mixing system during transitions up to the onset of steady state (Van Cruyningen et al., 1990; Unger and Muzzio, 1999; Law and Wang, 2000; Bruchhausen et al., 2005; Diez et al., 2005). With PLIF, a laser sheet is used to illuminate a planar cut of the flow field that has been seeded with a fluorescent tracer species. When the fluorescent species is a complex organic dye, the emitted light induced by the laser is relatively broadband. Under certain conditions (such as low dye concentration and low laser intensity), the intensity of the emitted light is proportional to the local concentration of the tracer species. The emitted light is then imaged by a high-resolution digital camera. In order to "freeze" the motion of the flow, a short-pulse pulsed laser is usually used. PLIF can be a useful technique for simple visualization of mixing processes but can be also used for quantitative concentration measurements. In principle high-resolution, high-speed imaging is possible, in which case this technique can be useful to analyze the time-evolution of the mixing process.

Kukura et al. (2003, 2004) utilized PLIF to investigate the hydrodynamics, as well as shear distribution and variability under turbulent conditions in the USP Dissolution Apparatus II. In these studies, the authors utilized rhodamine-B and rhodamine-wt as the dye tracers, which were injected at the bottom of the vessel and just above the paddle via a syringe to simulate the convection of an active ingredient from a dosage article, and to image the recirculation regions above and below the paddle. The dye transport during the experiment was consistent with the results of their PIV experiments. Non-uniform mixing characterized by zones of segregation was confirmed as the dye failed to penetrate upper regions of the dissolution vessel. These studies also demonstrated that PLIF is a viable method for analyzing the dynamic mixing patterns of the USP Dissolution Apparatus II.

The objective of this study was to utilize the PLIF technique to investigate the mixing patterns and pH neutralization during the buffer medium addition of the method A enteric test. Specifically, rhodamine-B dye solution was used to image the mixing of the buffer medium with the acid medium, and to quantitatively determine the time required for complete mixing of the two phases for different methods of buffer addition.

The pH-sensitive dye fluorescein was used to image the pH development during the neutralization step of the method A enteric test for different methods of buffer medium addition. Finally, tablets coated with Eudragit® L 30 D-55 containing rhodamine-B dye were used to discern any differences in polymer dissolution rate when tested according to method A with rapid buffer addition versus method B.

2. Materials and methods

2.1. Planar laser-induced fluorescence

The light source for the PLIF imaging was an acousto-optically Q-switched diode-pumped Nd:YAG laser (Coherent Inc. Corona) operated at 2000 pulses/s. The wavelength of the laser was 532 nm, the energy per pulse was about 13.5 mJ and the pulse duration was about 160 ns. The laser sheet was formed by using a plano-concave cylindrical lenses with a focal length of 12.7 mm and a plano-convex focusing lens with a focal length of 750 mm. The cylindrical lens was used to spread the beam into a sheet about 250 mm in height and the convex lens was used to focus the sheet to a thickness of about 1.2 mm. A CMOS digital camera (Photron APX) fitted with a 50 mm, f/1.4 lens was used for imaging. In order to eliminate scattered laser light from the images, the lens was fitted with a 570 nm longpass filter. The camera was operated at 10 Hz with a resolution of 1024 × 512 pixels (resolution in the physical plane of about 0.2 mm/pixel). Note that the laser was operated at a much higher frequency than the camera and so the camera detected only one out of every 200 pulses emitted by the laser.

A schematic diagram illustrating the equipment configuration for the PLIF imaging experiments performed in this study is shown in Fig. 1. The output from the laser was divided into two equal intensity beams by use of a 50/50 beam splitter. The resulting two beams were directed to opposite sides of the dissolution vessel. Both beams were formed into sheets with a combination of cylindrical and spherical lenses as shown. Two laser sheets were counterpropagating, parallel to each other and bisected the dissolution vessel such that they intersected the paddle or paddle shaft at opposite sides. The advantage of using two counterpropagating sheets in this way is that it enables the illumination of the entire vessel. With single-sheet illumination either one half of the vessel is obscured by the shadow cast by the shaft or the actual plane-of-symmetry cannot be imaged.

For all PLIF imaging experiments, a Vankel Vanderkamp 6000 model, 6-station dissolution system was used (Chatham, New Jersey). The water bath was removed from the machine in order to project the laser sheet through the dissolution vessel below the vessel support plate. The paddle speed for all experiments was 50 rpm.

2.2. Mixing profile imaging by PLIF with rhodamine-B

Rhodamine-B (Fluka Biochemika, Buchs, Switzerland), is a fluorescent dye with an absorption spectrum in the range of 450–580 nm with a peak value at 543 nm, and a broad emission spectrum that peaks at 564 nm when excited at 543 nm (Du et al., 1998). Rhodamine-B is a suitable dye for this study because its absorption spectrum includes the wavelength of the laser used for the PLIF imaging. A solution of rhodamine-B was used in this study to represent the buffer medium that is added to the acidic medium during the pH neutralization step of the method A procedure. Rhodamine-B was utilized only for visualization of fluid mixing patterns, and therefore deionized water was used to simulate both acid and buffer media phases since pH development was not of concern. Hence, 250 mL of aqueous rhodamine-B solution was added to 750 mL of pure deionized water in the dissolution vessel for each method of

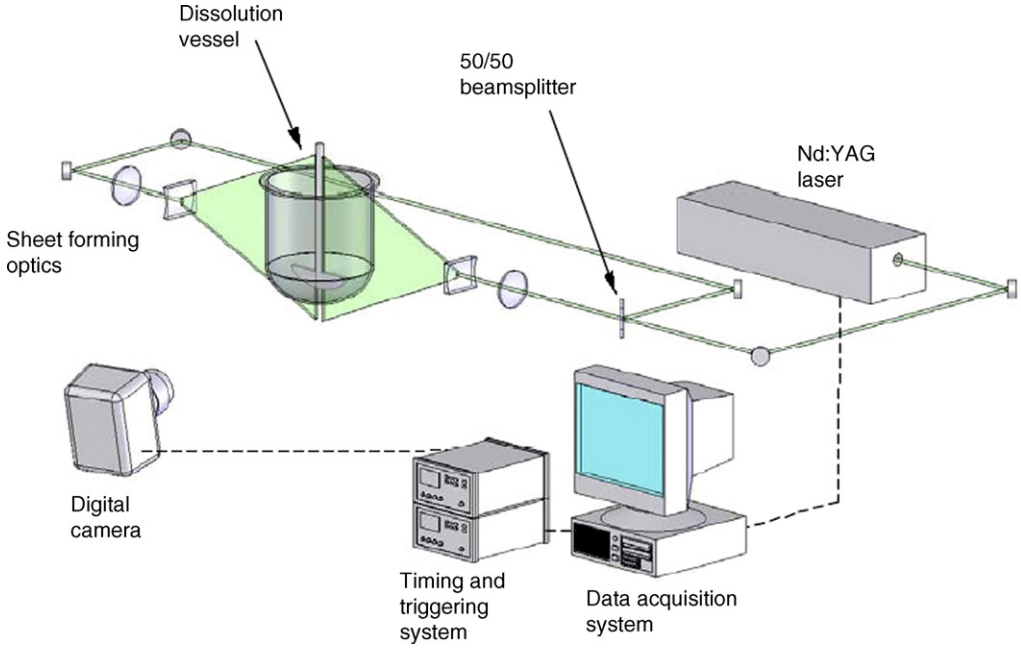

Fig. 1. Schematic diagram of the PLIF experimental set-up.

addition. The imaging of mixing patterns was done at ambient conditions as the effect of temperature (in the range of 25–37 °C) on the mixing of the two media is negligible in comparison to the large-scale stirring generated by the rotating paddle. For each of the mixing visualization experiments with rhodamine-B, the same PLIF experimental set-up and dissolution apparatus were used as mentioned above.

Three methods of buffer phase media addition were evaluated in this study: rapid addition, gradual addition along the paddle shaft, and gradual addition near the vessel wall. The USP states that the operation of adding the buffer phase and adjusting the pH must be completed within 5 min for the method A enteric test. The rapid and gradual methods of addition were designed to test the two extremes of this time constraint in order to determine how mixing of the media is affected by the rate of buffer phase addition. It is important to note that the gradual rate of addition is not intended to only represent the addition of 250 mL in exactly 5 min, but rather to generally illustrate a slow, drop-wise method of addition. For rapid addition, the 250 mL of buffer medium was poured from a graduated cylinder into the dissolution vessel containing the acid medium over a period of about 5 s. For the gradual addition methods, the 250 mL of buffer medium was added over about 5 min using a separatory funnel with a stopcock that was used to regulate the flow. The flow from the separatory funnel was directed to the targeted site of addition in the dissolution vessel by the use of silicone tubing. Gradual media addition near the paddle shaft and near the vessel walls were investigated to determine if mixing of the two phases is dependent on the location of addition within the dissolution vessel when the buffer media is added slowly to the acidic media.

2.3. pH development imaging by PLIF with fluorescein dye

Method A involves chemically reacting flow resulting from the mixing of a strongly basic buffer solution with a strongly acidic solution. The most commonly used technique to non-intrusively visualize mixing during acid–base reactions are simple pH indicators (Lamberto et al., 1996; Johari and Paduano, 1997; Lamberto et al., 1999). Laser-induced fluorescence of pH sensitive dyes has been used extensively for this purpose (Dahm and Dimotakis, 1990; Coppeta and Rogers, 1998). For this study, fluorescein was employed to visualize the pH evolution during the mixing process.

The fluorescence intensity of laser grade fluorescein (Acros Organics, Geel, Belgium) is dependent on the pH of the dilution medium (Klonis and Sawyer, 1996). Fluorescein shows increased fluorescence with increasing pH over a range of about 5–9. In this range of pH, by proper calibration, it is possible to estimate the distribution of pH in the flow field (Coppeta and Rogers, 1998). For these experiments, equal concentrations (3×10^{-5} M) of fluorescein dye were used in both the buffer phase and the acid phase media. In this way, differences in fluorescence intensity seen during the evolution of the mixing process are entirely due to pH differences rater than differences in fluorescein concentration. The acid and buffer media were used as stipulated by the USP for the method A enteric test. Hence, 250 mL of 0.2 M sodium phosphate tribasic buffer containing fluorescein dye was added to 750 mL of 0.1N HCl, also containing fluorescein dye in the same concentration, for each mixing experiment. Both phases were heated to 37 ± 0.5 °C prior to the start of the imaging process. The three methods of buffer medium addition mentioned above were also utilized in this case; however, in the case of the two of gradual buffer addition methods, a peristaltic pump was used to accurately deliver 50 mL/min of the buffer phase to the dissolution vessel over a period of 5 min. The buffer media was directed to the targeted site via silicone tubing. The PLIF configuration and the dissolution equipment were used as stated above.

2.4. Image and data processing

The raw PLIF images obtained during the experimental procedure were processed in order to remove the effects of: (1) spatial variations in the laser sheet intensity, (2) camera dark noise, and (3) interference from background reflections of the laser light. Additionally, the pH measurements required certain calibration procedures as detailed below. Both the PLIF images obtained with rhodamine-B and with fluorescein dyes where corrected for background noise and laser sheet non-uniformities according to the methodology described by Clemens (2002). In order to quantitatively analyze the results obtained from PLIF with rhodamine-B, the images were normalized by the fluorescence intensity of the pure "buffer medium" before addition to the dissolution vessel. The resulting relative fluorescence signal is equal to the volume-fraction of buffer medium in the probe volume and is termed the "mixture fraction." Since the proportions of buffer to acid media were 1:3, the final (well-mixed) state has a mixture fraction of 0.25.

The same scaling procedure was applied to the imaging studies with fluorescein; however, in the case of a pH-sensitive dye, normalization to the final well mixed state relates to a pH value rather than a concentration. Therefore, a value of unity on the normalized scale corresponds to the pH of the media upon complete mixing, and values greater or lesser than unity represent higher and lower pH values, respectively. In order to assign pH values to the normalized scale, a calibration curve was generated relating illumination intensity of fluorescein to the pH of the dissolution medium by imaging a series of fluorescein containing buffer solutions of known pH and then normalizing those images by the image with a pH equal to the experimental dissolution medium after complete mixing. The normalized fluorescence intensity was then plotted versus pH to generate the calibration curve shown in Fig. 2. Fluorescein dye exhibits temperature dependent fluorescence, and therefore the calibration curve was generated at 37 °C in order to accurately assign pH values to the experimental images. The investigated pH range included pH 5.0 through 8.0. Below a pH of 5.0, almost no light emission was detected, and above pH 8.0 there was essentially no difference in illumination intensity; therefore, no indication of pH can be determined below pH 5.0 or above 8.0 with the fluorescein dye used in this experiment. The obtained data points were fit to an error function that was used to generate the normalized pH color map that was then applied to the experimental images. With this calibration curve, the fluorescein excitation

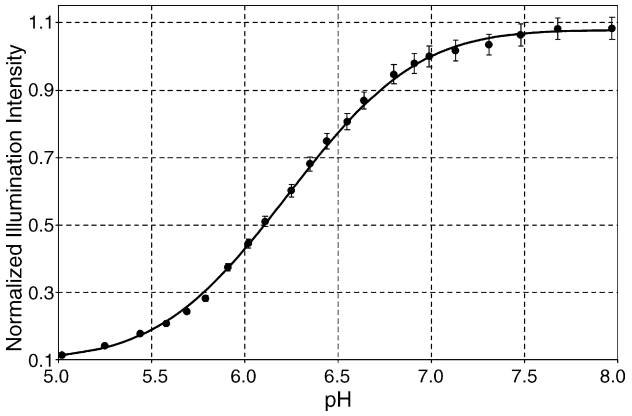

Fig. 2. Calibration curve relating normalized illumination intensity of fluorescein to the pH of the buffer media.

at any point in an experimental image can be converted to its corresponding pH value.

The uncertainty on the calibration curve is estimated to be less than ±6% over the full range of pH. The primary source of this uncertainty is absorption of the laser light by the fluorescein molecules as the laser sheet transverses the vessel. This results in decreased illumination intensity along the path length of the laser sheet as it is projected through the vessel. Therefore, a low concentration of fluorescein dye (9×10^{-6} M) was used in order to minimize absorption. The difference in dye concentration between the calibration curve imaging and the experimental imaging does not impact the results as differences in concentration are canceled out by the normalization process described above. Moreover, the dual laser sheet configuration of the experimental PLIF set-up also acts to decrease the uncertainty due to absorption by reducing the path length of the projected laser sheet by about one half when compared to a single laser sheet projected over the entire width of the vessel.

2.5. Unmixedness

In order to quantitatively illustrate the progression of mixing in the dissolution vessel, a quantity termed the "unmixedness" was used. The unmixedness is a measure of the large-scale spatial non-uniformity of the buffer throughout the dissolution vessel and is defined as follows. A total of 30 discrete regions, each 7×7 pixels in area ($\sim 1.4 \times 1.4$ mm^2), were selected to represent the concentration of rhodamine-B dye at various points distributed throughout the dissolution vessel. The distribution of these 30 discrete regions in the dissolution vessel is depicted in Fig. 3. The mean fluorescence intensity for the 49 pixels within each point was calculated along with the standard deviation between the 30-point means for each image in the mixing sequence. The unmixedness is defined as the standard deviation of the 30 points normalized by the mean value of these same points. If the different points have largely different concentrations then the unmixedness will be large, whereas uniform mixing leads to an unmixedness of 0. The unmixedness was calculated every tenth of a second for the entire media addition process.

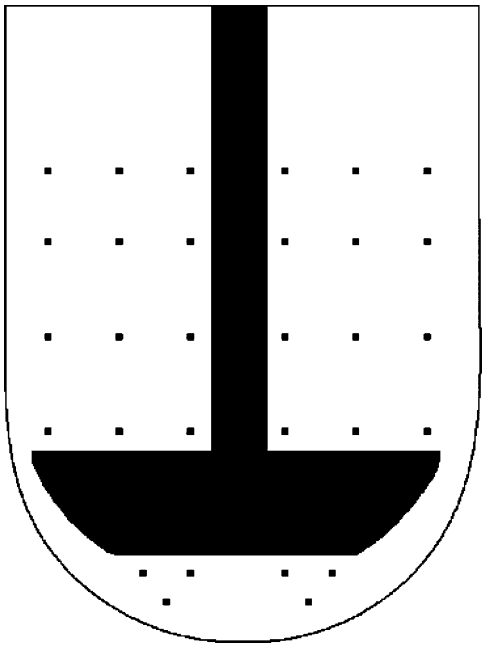

Fig. 3. Schematic representation of the distribution of the discrete areas in the dissolution vessel used to calculate unmixedness with time for the mixing pattern visualization with rhodamine-B solution.

2.6. Comparison of enteric polymer dissolution with methods A and B

For these studies, a placebo core tablet was manufactured and coated with an Eudragit® L 30 D-55 dispersion (Degussa, Darmstadt, Germany) containing rhodamine-B dye. Each tablet contained approximately 1 mg of rhodamine-B in the film coating. Using PLIF, the dissolution of the rhodamine-containing enteric coat was observed. As the enteric coating dissolved, the rhodamine-B contained in the coat was released and the fluorescence was imaged. By imaging the release of rhodamine-B from the coat, the polymer dissolution rate for method A with rapid buffer addition and Method B enteric tests could be compared. The tablets were first tested in acid to ensure that rhodamine-B remains in the film until the onset of polymer coat dissolution. For method B, the tablet was placed in buffer medium at a pH of 6.8. For method A, the tablet was first immersed in the acid medium followed by the rapid addition of buffer medium. The initiation of imaging (time = 0) for method B began when the tablet had settled to the bottom of the dissolution vessel. For method A, the initiation of imaging began at the moment when the buffer phase addition was completed.

3. Results and discussion

3.1. Imaging of mixing development with rhodamine-B—rapid media addition

Fig. 4 shows a series of images that illustrate the mixing pattern for the rapid addition of 250 mL of rhodamine-B solution to 750 mL of water which was used to represent the addition of the buffer medium to the acid medium for the method A enteric test.

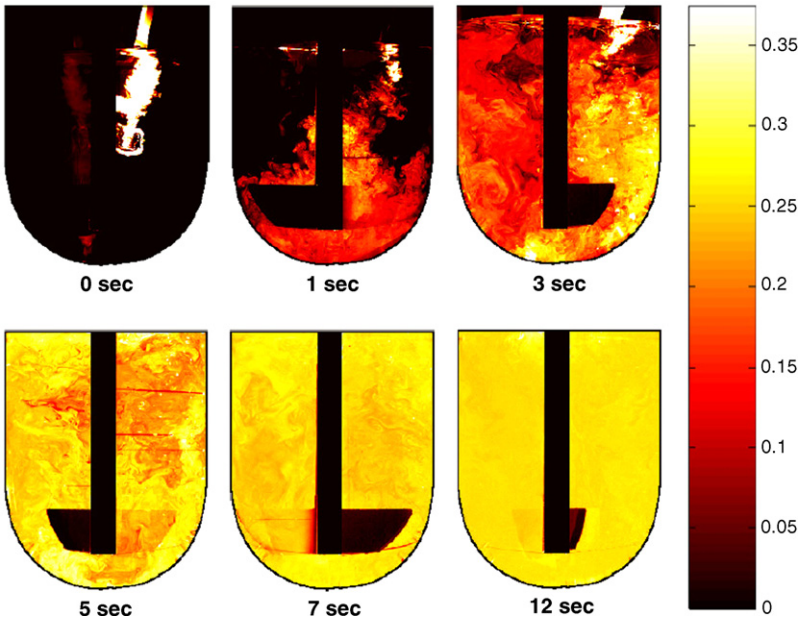

Fig. 4. Time-sequence of the mixture fraction field for rapid addition of rhodamine-B dye solution.

It can be seen from the first image in the sequence that as the rhodamine-B solution enters the vessel it has a high concentration since little mixing has occurred. The colormap is limited to values of the mixture fraction below 0.375 so that the lower concentration regions are more easily visualized. One second after the start of buffer medium addition, the mixing effects of the paddle can be seen as the highly concentrated dye solution descends into the vortex near the paddle blade and is rapidly dispersed by the paddle's rotation. By comparing the motion of the dye solution from the 3-s image to the 5-s image, the flow pattern created by the rapid pouring of the secondary media can be seen. From the pouring of the rhodamine-B solution, a circular mixing pattern develops as the medium descends down the wall of the vessel nearest to the point of entry and then follows the contour of the vessel as it moves along the bottom and ascends up the opposite vessel wall. This large-scale stirring results from the addition of the descending high-momentum secondary medium and is separate from the stirring generated by the paddle. The result is that the rhodamine-B solution is rapidly dispersed throughout the vessel, most importantly to areas within the vessel that are not well mixed by the rotation of the paddle. The rapid pouring of the secondary medium also creates substantial turbulence within the vessel, which can be seen by the formation of small eddies throughout the vessel. The secondary media addition was completed in about 5 s; thus it can be seen from the image at 7 s that 2 s after complete addition of the secondary media, the system is rapidly approaching homogeneity. The final image in the sequence shows that after 12 s from the start of addition the system has reached almost complete equilibrium.

The rapid pouring of the secondary media increases both the large-scale stirring and small-scale turbulence. The large-scale stirring enables the transport of high mixture fraction fluid from one side of the vessel to the other, and thus reduces the global inhomogeneity of the flow. It is well known that small-scale turbulent eddies act to stretch intermaterial surfaces, which leads to larger intermaterial surface areas and larger concentration gradients, both of which lead to enhanced rates of diffusion (Ranz, 1979, 1985). Therefore, rapid addition of the "buffer phase" to the "acid phase" results in efficient mixing of the two phases by increasing large-scale transport of the buffer and the rate of diffusion within the vessel.

Fig. 5 shows the time-evolution of the unmixedness for the rapid addition of the rhodamine-B solution. Recall that the unmixedness is a measure of the global inhomogeneity of the mixture over the entire dissolution vessel. It can be seen from this figure that initially the unmixedness exceeds 250%, which indicates that there are significant large-scale concentration differences in the vessel prior to the development of the circulating flow pattern generated by the rapid addition of the secondary media. During the first few seconds of addition there are areas of extreme concentration differences as domains of high dye concentration have yet to be convected to areas of the dissolution

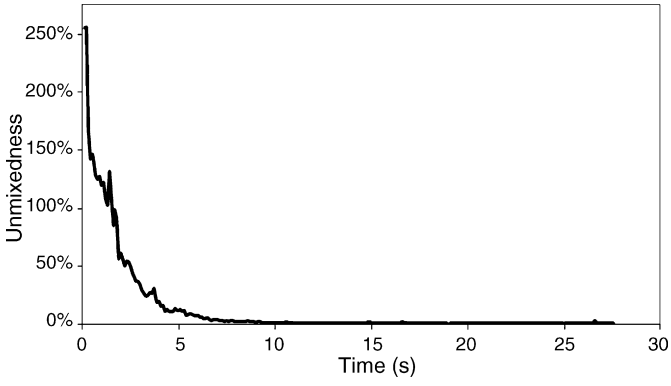

Fig. 5. Time evolution of the unmixedness for the rapid addition of rhodamine-B dye solution.

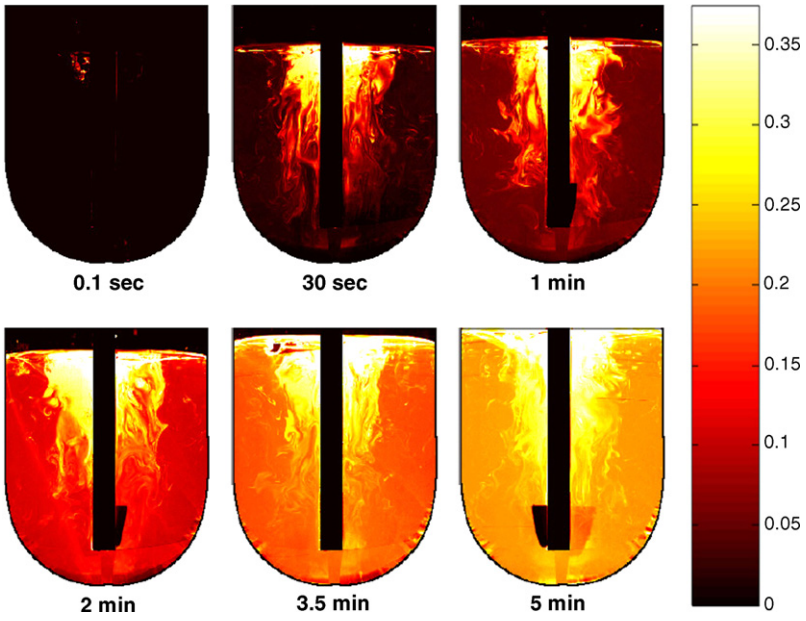

Fig. 6. Time-sequence of the mixture fraction field for gradual addition of rhodamine-B solution near the paddle shaft.

vessel where the agitation due to the paddle is minimal, namely the upper portions of the vessel. Once the circulatory mixing pattern develops, the concentration deviations in the vessel are rapidly diminished as dye is convected to the more stagnant regions of the vessel. Consequently, at the completion of media addition (5 s), the unmixedness is reduced to 19%. After 7.5 s from the start of addition, the unmixedness within the vessel is approximately 3%, indicating that uniformity, on the scale of the point areas ($\sim 1.4 \times 1.4\,mm^2$), occurs rapidly following convection of the dye throughout the vessel. This figure demonstrates that rapid addition of the buffer medium to the acid medium results in efficient mixing of the two phases and indicates that the probability of developing hot spots with rapid buffer addition during the neutralization step of the method A enteric test is very low.

3.2. *Imaging mixing development with rhodamine-B solution—gradual media addition*

The time-sequence of images shown in Fig. 6 illustrates the mixing pattern for the gradual addition of the secondary media directed near the shaft of the paddle. It can be seen from this sequence of images, that there is substantial segregation of the dye solution in a conical region around the paddle shaft that elongates over the course of the media addition. Segregation in this region is expected as Muzzio and coworkers have shown that a low velocity recirculation region is formed in this area by the rotation of the paddle (Kukura et al., 2003, 2004; Baxter et al., 2005). In this region of the vessel, convective stirring is low, and thus the rhodamine-B solution appears to stagnate, particularly near the liquid surface. Since the rate of addition is relatively slow, the momentum of the rhodamine-B solution droplets entering the primary media is not sufficient for transport out of the recirculation region. The large-scale segregation of the dye persists to over 5 min.

Fig. 7 shows the unmixedness over the entire time required for secondary media addition. Initially the unmixedness exceeds 500%, it then decreases to about 50% after 100 s of addition time, and further decreases to 13% after 5 min of mixing time. This illustrates that the movement of dye from the vortex region occurs relatively slowly over a period of several minutes, during which there exists substantial concentration differences within the vessel. Therefore, it can be expected that slow addition of the buffer phase at the paddle shaft for the method A enteric test will result in high pH regions in the vortex at the center of the dissolution vessel, and overall poor homogeneity of the mixing system during the addition process. This is an undesirable mixing profile as it could lead to variations in the performance of the tested enteric dosage form.

In the investigation of the mixing profile for the gradual media addition, the influence of the location of media addition was also investigated by examining the effect of adding the secondary

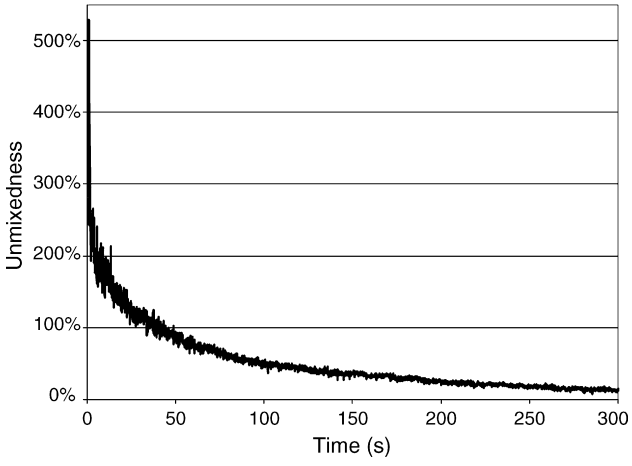

Fig. 7. Time evolution of the unmixedness for the gradual addition of rhodamine-B dye solution near the paddle shaft.

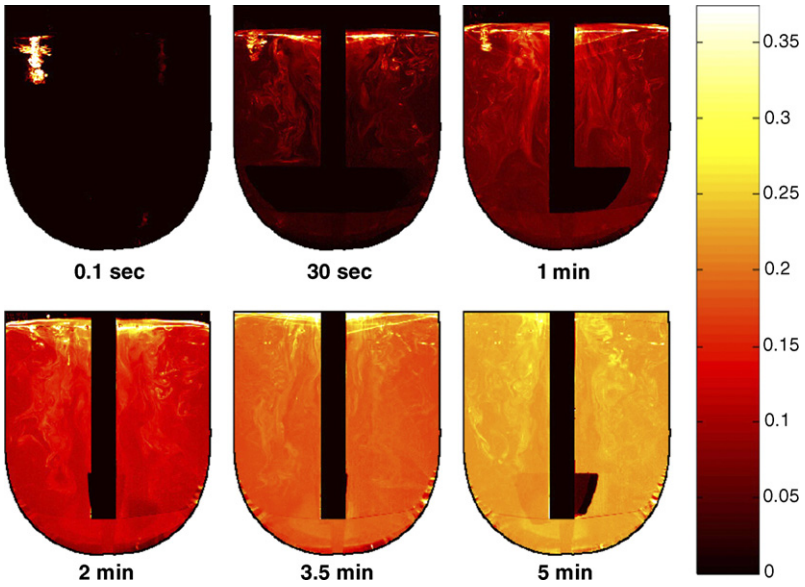

Fig. 8. Time-sequence of the mixture fraction field for gradual addition of rhodamine-B solution near the vessel wall.

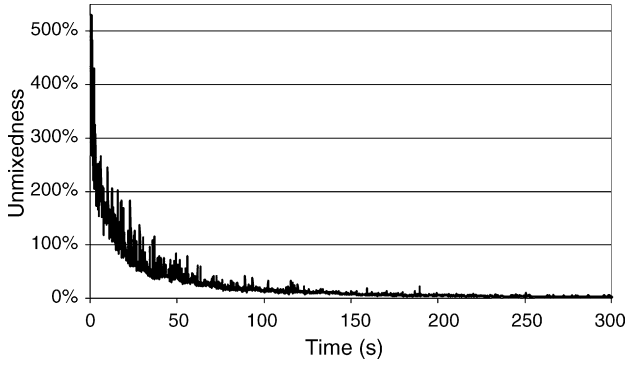

Fig. 9. Time evolution of the unmixedness for gradual addition of rhodamine-B dye solution near the vessel wall.

media near the vessel wall rather than along the paddle shaft. Fig. 8 shows a sequence of images depicting the evolution of mixing over 5 min of simulated buffer medium addition. It can be seen from this series of images that the problem of segregation of the dye solution along the paddle shaft is largely eliminated by adding the media near the wall of the dissolution vessel. Muzzio and coworkers have shown that the rotation of the paddle generates circular mixing patterns of ascending and descending flow along the walls of the dissolution vessel (Kukura et al., 2003, 2004). The slow addition of the secondary media at these higher shear regions allows the droplets to be more readily convected from the liquid surface to lower regions in the vessel by becoming entrained in the circulating flow along the walls. In addition, the high shear flow near the walls also acts to stretch

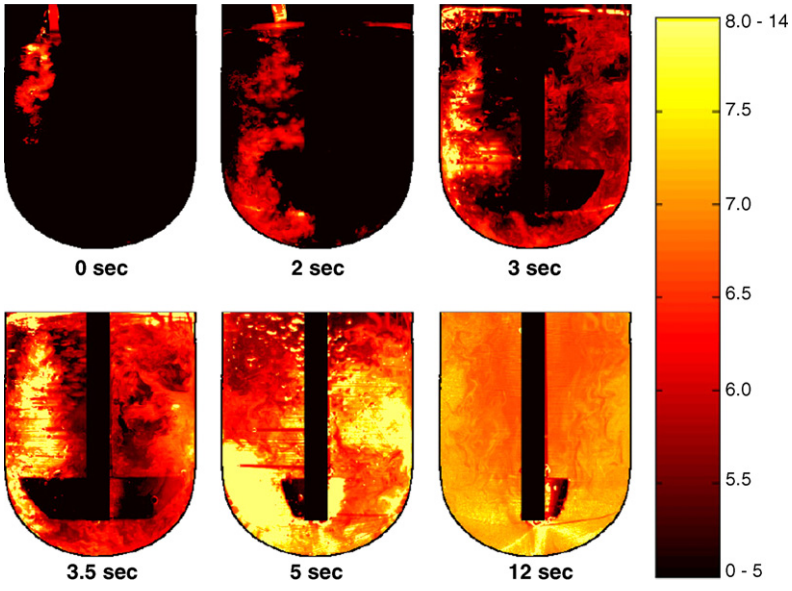

Fig. 10. Time-sequence of the pH development field for rapid addition of 0.2 M sodium phosphate tribasic (50 mL/s).

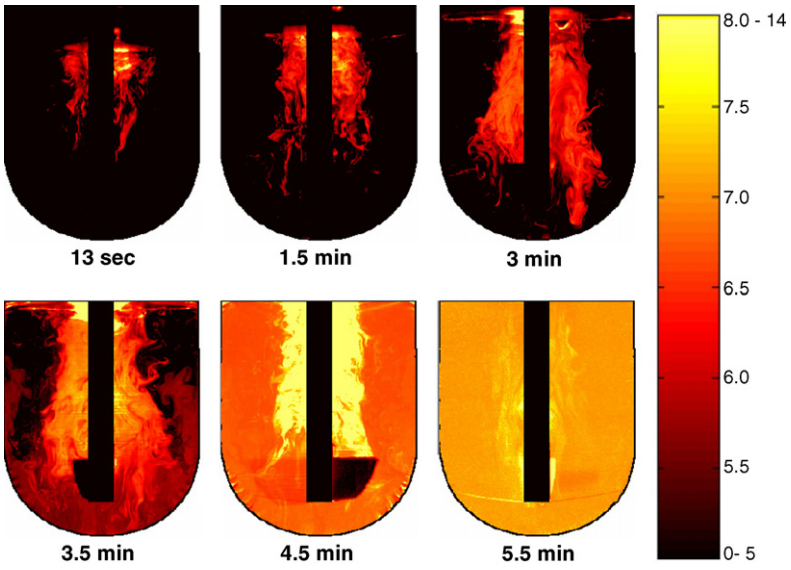

Fig. 11. Time-sequence of the pH development field for gradual addition of 0.2 M sodium phosphate tribasic near the paddle shaft (50 mL/min).

and deform the droplets as they enter the primary media such that the interfacial area and concentration gradient increase substantially, thereby improving the rate of diffusion. Consequently, the mixing of the rhodamine-B solution occurs more rapidly when the secondary media is added slowly near the wall rather than along the paddle shaft due to increased convection and improved diffusion.

Fig. 9 depicts the time evolution of the unmixedness for the slow media addition at the vessel wall. It is seen that initially the unmixedness is similar to the media addition at the shaft. This is due to the fact that the convective motions near the vessel wall are relatively weak, and thus transport of the dye to the lower regions of the vessel is somewhat slow. Although the initial concentration differences are similar, it can be seen that with gradual addition near the vessel wall the unmixedness decreases much more rapidly than with addition near the shaft. This further indicates that convective mixing and shearing of the secondary media droplets by the circulating flow patterns near the vessel wall results in more rapid mixing when compared to addition of the media at the paddle shaft. Therefore, if slow media addition is required or preferred for a particular test method, the media addition should be made near the vessel wall as it results in more efficient mixing.

3.3. pH development with fluorescein dye

As shown in Fig. 10, the rapid addition of the 250 mL of buffer medium to the acid medium over 5 s exhibits a similar flow pattern as seen with the rhodamine-B mixing study. As stated above, the convective mixing and turbulence generated by the circulating flow pattern, as well as the increased shear allowed for rapid mixing of the two phases and accelerated the

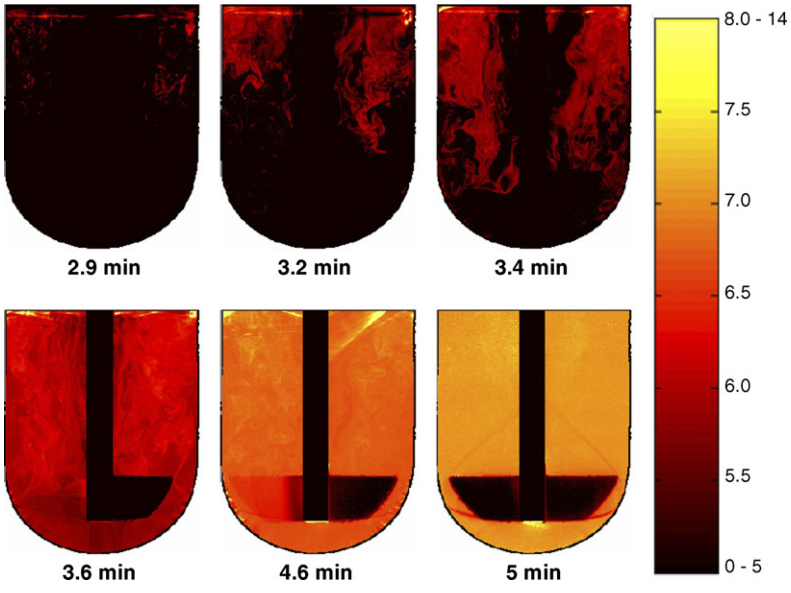

Fig. 12. Time-sequence of the pH development field for gradual addition of 0.2 M sodium phosphate tribasic near the vessel wall (50 mL/min).

neutralization reaction. There were no stagnant regions of high pH detected during the mixing process. Complete neutralization of the system pH was achieved after about 20 s.

Slow addition of the buffer medium over 5 min at a rate of 50 mL/min near the paddle shaft resulted in segregation as illustrated in Fig. 11. Soon after the start of the buffer addition, a vortex region of higher pH developed and stagnated around the paddle shaft. After about 3 min, the vortex elongated to reach the paddle blade, at which point the high pH media began to disperse to the regions of the vessel below the paddle and near the walls. The neutralization reaction was completed after 5.5 min, a slightly longer period than the time of addition. Again, the pH development followed a similar trend as seen with the rhodamine-B mixing studies. The low fluid velocity and shear forces in the vortex region hinder the transport of the high pH medium to other regions in the vessel and reduces the rate of diffusion. Consequently, the vortex region near the paddle becomes a recirculation region of high pH during the buffer addition process for this method of addition.

As seen with the rhodamine-B mixing studies, the segregation in the vortex was improved by directing the gradual buffer addition to an area near the vessel wall as shown in Fig. 12. The circulating flow pattern near the wall of the vessel generated by the paddle provides improved mixing by increasing convection and shear of the buffer phase droplets which correspondingly increases the rate of pH neutralization. Up to 3 min after the beginning of buffer addition, there is no fluorescence detectable as the pH of the entire dissolution vessel is below 5. Between 3 and 4 min, the sudden color change represents the onset of fluorescence at a pH of about 5.5 in the area of the circulating flow between the vessel wall and the paddle shaft. Complete pH neutralization occurred simultaneously with the end of the alkaline medium addition after 5 min.

3.4. Comparison of enteric polymer dissolution with methods A and B

It was demonstrated in the previous sections that a large and sustained hot spot was generated by gradual addition of the buffer medium down the paddle shaft. It was also shown that by altering the location of gradual buffer addition, the mixing efficiency was substantially improved and hot spot generation was eliminated. This suggests that gradual buffer addition near the paddle shaft is not a valid method of addition, while gradual addition near the vessel wall is an ideal method of buffer medium addition. Although it was demonstrated that rapid buffer addition was very efficient with respect to mixing and pH neutralization, it was also observed that the rapid pouring action caused the buffer medium to pass first through the lower regions before being dispersed throughout the remainder of the vessel. This flow pattern causes a substantial fraction of somewhat unmixed buffer medium to briefly traverse the region where a typical dosage form would reside during testing. Although too brief to be considered a hot spot, this consequence of rapid buffer addition must be further investigated to determine its effect on the dissolution of an enteric-coat in order to fully validate this method of addition. To this end, placebo tablets coated with Eudragit® L

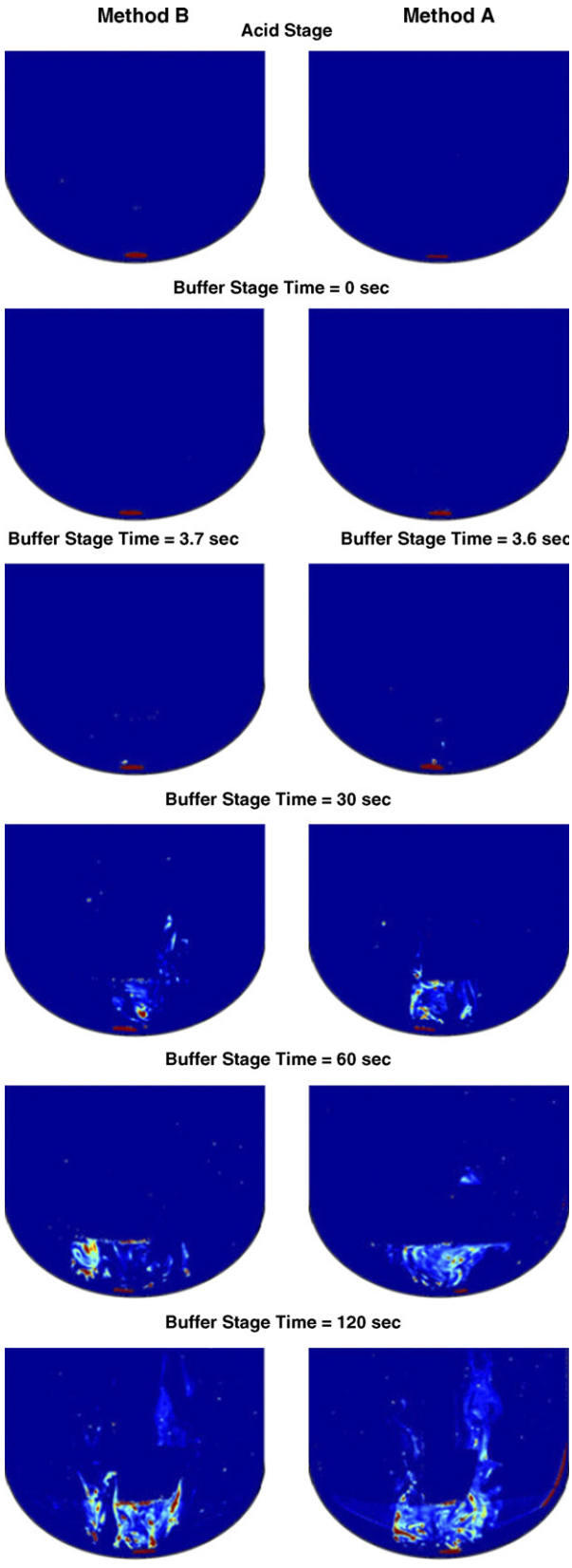

Fig. 13. PLIF images of tablets coated with Eudragit L 30 D-55 containing rhodamine-B tested for enteric dissolution performance according to USP methods A and B.

30 D-55 containing rhodamine-B were used to visualize the dissolution of an enteric-coat in order to determine if rapid buffer addition accelerates the polymer dissolution rate. As a comparison, these tablets were also subjected to the USP method B enteric test.

Fig. 13 shows the resulting images from both test methods at specific time points. Initially, the tablets appear bright red due to the fluorescence of the rhodamine-B contained in the coat. As the enteric coat dissolves, rhodamine-B is released into the media thereby allowing for visualization of the polymeric coat dissolution. The tablets tested in both cases showed no release of rhodamine-B from the enteric coat during the acid stage confirming that rhodamine-B is not released from the film prior to dissolution of the enteric coat. The images taken at the zero time point show that there is no instantaneous dissolution of the film coat using either enteric method. This demonstrates that the rapid addition of buffer medium with method A did not expose the tablets to elevated pH for a sufficient time to elicit a burst release of rhodamine-B from the enteric coat. The images labeled 3.6 s (method A) and 3.7 s (method B) represent the onset of enteric coat dissolution and indicate that the initiation of polymer dissolution is very similar in both cases. Further dissolution of the tablet coatings is observed as the test continues over 2 min. The rate of dissolution of the polymer coatings and subsequent release of rhodamine-B appear to be very similar for both test methods. Thus, this study indicates that there is essentially no difference in the dissolution rate of an Eudragit® L 30 D-55 enteric-coated dosage form when tested for enteric performance according to method A with rapid buffer addition as compared to method B.

4. Conclusions

The results of the investigation of the USP drug release standard for enteric-coated articles method A with rhodamine-B and fluorescein dyes demonstrate that the mixing profiles and pH development follow similar trends for all methods of addition studied. Rapid addition of the buffer medium to the acid medium produced the most efficient mixing and pH neutralization as a result of increased stirring (convection) and turbulence resulting from the addition of the high momentum buffer media into the stationary acidic media. For the gradual methods of buffer medium addition, the efficiency of mixing and pH neutralization was seen to be location dependent as a result of the heterogeneous flow patterns generated in the dissolution vessel by the rotating paddle. Addition of the buffer medium along the paddle shaft results in inefficient mixing and pH neutralization due to segregation of the added media in the recirculating region that surrounds the paddle shaft. In contrast, introducing the buffer media slowly near the wall of the vessel shows more efficient mixing and pH neutralization as a result of more rapid dispersion of the droplets by the large-scale vortical motions that exist near the vessel walls. Enteric-coated tablets tested by the method A enteric test with rapid buffer medium addition and the method B enteric test exhibited very similar enteric polymer dissolution rates, thus indicating that the rapid addition of highly basic media to the acid phase does not influence the result of the method A enteric test. From the results of the PLIF imaging studies with rhodamine-B, fluorescein, and enteric-coated tablets, it was seen that "hot spots" affecting the dissolution performance of enteric-coated dosage forms are not generated during the neutralization step of the method A enteric test when the media is added rapidly or outside of the low-shear vortex region that surrounds the paddle shaft.

References

Alavi, A.K., Squillante III, E., Mehta, K.A., 2002. Formulation of enterosoluble microparticles for an acid labile protein. J. Pharm. Pharmaceut. Sci. 5, 234–244.

Baxter, J.L., Kukura, J., Muzzio, F.J., 2005. Hydrodynamics-induced variability in the USP apparatus II dissolution test. Int. J. Pharmaceut. 292, 17–28.

Beckett, A., Quach, T., Kurs, G., 1996. Improved hydrodynamics for USP Apparatus 2. Dissol. Technol. 3, 7–18.

Bruce, L.D., Koleng, J.J., McGinity, J.W., 2003a. The influence of polymeric subcoats and pellet formulation on the release of chlorpheniramine maleate from enteric coated pellets. Drug Dev. Ind. Pharm. 29, 909–924.

Bruce, L.D., Petereit, H.-U., Beckert, T., McGinity, J.W., 2003b. Properties of enteric coated sodium valproate pellets. Int. J. Pharmaceut. 264, 85–96.

Bruchhausen, M., Guillard, F., Lemoine, F., 2005. Instantaneous measurement of two-dimensional temperature distributions by means of two-color planar laser-induced fluorescence (PLIF). Exp. Fluids 38, 123–131.

Clemens, N.T., 2002. Flow imaging. In: Hornak, J.P. (Ed.), Encyclopaedia of Imaging Science and Technology. John Wiley & Sons, New York.

Coppeta, J., Rogers, C., 1998. Dual emission laser-induced fluorescence for direct planar scalar behavior measurements. Exp. Fluids 25, 1–15.

Crotts, G., Sheth, A., Twist, J., Ghebre-Sellassie, I., 2001. Development of an enteric coating formulation and process for tablets primarily composed of a highly water-soluble, organic acid. Eur. J. Pharmaceut. Biopharmaceut. 51, 71–76.

Dahm, W.J.A., Dimotakis, P.E., 1990. Mixing at large Schmidt number in the self-similar far field of turbulent jets. J. Fluid Mech. 217, 299–330.

Diez, F.J., Bernal, L.P., Faeth, G.M., 2005. PLIF and PIV measurements of the self-preserving structure of steady round buoyant turbulent plumes in crossflow. Int. J. Heat Fluid Flow 26, 873–882.

Du, H., Fuh, R.A., Li, J., Corkan, A., Lindsey, J.S., 1998. PhotochemCAD: a computer-aided design and research tool in photochemistry. Photochem. Photobiol. 68, 141–142.

Felton, L.A., Haase, M.M., Shah, N.H., Zhang, G., Infeld, M.H., Malick, A.W., McGinity, J.W., 1995. Physical and enteric properties of soft gelatin capsules coated with Eudragit® L 30 D-55. Int. J. Pharmaceut. 113, 17–24.

Fuerst, T., Bott, C., Stein, J., Dressman, J.B., 2005. Enteric-coated cholylsarcosine microgranules for the treatment of short bowel syndrome. J. Pharm. Pharmacol. 57, 53–60.

Genc, L., Guler, E., Hegazy, N., 1997. Film-coated enteric tablet formulation of ketorolac tromethamine. Drug Development and Industrial Pharmacy 23, 1007–1011.

Hanson, R., Gray, V., 2004. Handbook of Dissolution Testing, 3rd ed. Dissolution Technologies, Inc., Hockessin, Delaware.

Hasan, M., Najib, N., Suleiman, M., El-Sayed, Y., Abdel-Hamid, M., 1992. In vitro and in vivo evaluation of sustained-release and enteric-coated microcapsules of diclofenac sodium. Drug Dev. Ind. Pharm. 18, 1981–1988.

Johari, H., Paduano, R., 1997. Dilution and mixing in an unsteady jet. Exp. Fluids 23, 272–280.

King, P.G., 1996. Altered dynamics for USP Apparatus 2. Dissol. Technol. 3, 8–13.

Klonis, N., Sawyer, W.H., 1996. Spectral properties of the prototropic forms of fluoroscein in aqueous solution. J. Fluoresc. 6, 147–158.

Kukura, J., Arratia, P.E., Szalai, E.S., Muzzio, F.J., 2003. Engineering tools for understanding the hydrodynamics of dissolution tests. Drug Dev. Ind. Pharm. 29, 231–239.

Kukura, J., Baxter, J.L., Muzzio, F.J., 2004. Shear distribution and variability in the USP Apparatus 2 under turbulent conditions. Int. J. Pharmaceut. 279, 9–17.

Lamberto, D.J., Alvarez, M.M., Muzzio, F.J., 1999. Experimental and computational investigation of the laminar flow structure in a stirred tank. Chem. Eng. Sci. 54, 919–942.

Lamberto, D.J., Muzzio, F.J., Swanson, P.D., Tonkovich, T.L., 1996. Unsing time-dependent RPM to enhance mixing in stirred vessels. Chem. Eng. Sci. 51, 733–741.

Law, A.W.-K., Wang, H., 2000. Measurement of mixing processes with combined digital particle image velocimetry and planar laser-induced fluorescence. Exp. Thermal Fluid Sci. 22, 213–229.

Mirza, T., Joshi, Y., Liu, Q., Vivilecchia, R., 2005. Evaluation of dissolution hydrodynamics in the USP, peak and flat-bottom vessels using different solubility drugs. Dissol. Technol. 12, 11–16.

Morihara, M., Aoyagi, N., Kaniwa, N., Katori, N., Kojim, S., 2002. Hydrodynamic flows around tablets in different pharmacopeial dissolution tests. Drug Dev. Ind. Pharm. 28, 655–662.

Qureshi, S.A., Shabnam, J., 2001. Cause of high variability in drug dissolution testing and its impact on setting tolerances. Eur. J. Pharmaceut. Sci. 12, 271–276.

Ranz, W.E., 1979. Applications of a stretch model to mixing, diffusion, and reaction in laminar and turblent flows. AIChE J. 25, 41–47.

Ranz, W.E., 1985. Fluid mechanical mixing—lamellar description. In: Ulbrecht, J.J., Patterson, G.K. (Eds.), Mixing of Liquids by Mechanical Agitation. Gordon and Breach Science Publishers, New York, pp. 1–28.

Schmid, S., Wahl, M.A., Schmidt, P.C., 2000. Enteric coating of ibuprofen crystals using modified methacrylate copolymers. Pharmazeutische Industrie 62, 635–641.

Thoma, K., Bechtold, K., 1999. Influence of aqueous coatings on the stability of enteric coated pellets and tablets. Eur. J. Pharmaceut. Biopharmaceut. 47, 39–50.

Unger, D.R., Muzzio, F.J., 1999. Laser-induced fluorescence technique for the quantification of mixing in impinging jets. AIChE J. 45, 2477–2486.

Van Cruyningen, I., Lozano, A., Hanson, R.K., 1990. Quantitative imaging of concentration by planar laser-induced fluorescence. Exp. Fluids 10, 41–49.

Williams, R.O., 2001. The influence of plasticizer on heat-humidity curing of cellulose acetate phthalate coated beads. Pharmaceut. Dev. Technol. 6, 607–619.

Yoo, M.K., Choi, H.K., Kim, T.H., Choi, Y.J., Akaike, T., Shirakawa, M., Cho, C.S., 2005. Drug release from xyloglucan beads coated with Eudragit for oral drug delivery. Arch. Pharmacol. Res. 28, 736–742.